International Journal of Architectural, Civil and Construction Sciences
ISSN: 2415-1734
Vol:5, No:11, 2011

Lateral Behavior of Concrete

Ali Khajeh Samani, Mario M. Attard

***Abstract*—**Lateral expansion is a factor defining the level of confinement in reinforced concrete columns. Therefore, predicting the lateral strain relationship with axial strain becomes an important issue. Measuring lateral strains in experiments is difficult and only few report experimental lateral strains. Among the existing analytical formulations, two recent models are compared with available test results in this paper with shortcomings highlighted. A new analytical model is proposed here for lateral strain axial strain relationship and is based on the supposition that the concrete behaves linear elastic in the early stages of loading and then nonlinear hardening up to the peak stress and then volumetric expansion. The proposal for the lateral strain axial strain relationship after the peak stress is mainly based on the hypothesis that the plastic lateral strain varies linearly with the plastic axial strain and it is shown that this is related to the lateral confinement level.

***Keywords*—**Confined Concrete, Lateral Strain, Triaxial test, Post peak behavior

I. Introduction

A key parameter in understanding concrete response to compressive stress and deformation is the lateral strain behaviour. Through a well established lateral strain axial strain relationship, the changing response of concrete from elastic to inelastic and the formation of macro-cracks can be understood. The accurate method to predict the confinement level in columns confined by reinforcement or FRP wraps is using the lateral strain versus axial strain relationship. ([1-4])

Use of a more accurate method in predicting the confinement level becomes more important in reinforced high strength concrete columns, where the confining ties are typically not at yield when the column reaches its maximum carrying load capacity. This phenomenon therefore nullifies many confinement models, which calculate the confinement level mainly by the assumption that the ties are at yield at the peak load. To solve this issue, using the lateral expansion of column to calculate the column confinement level has become a common practice in recent years. Therefore the importance of a precise lateral strain versus axial strain relationship is more noticeable.

In this paper, two lateral strain versus axial strain models are reviewed and later on compared with experimental results besides a new model is proposed. The model is based on the hypothesis that concrete behaves linearly elastic to a certain limit observed by [5]. It has been shown[6] that the expansion of a concrete specimen starts at the peak stress level or its vicinity. Therefore this property is used to predict the lateral strain at the peak level. The last benchmark in predicting the lateral strain is the relationship of the plastic lateral strain with the plastic axial strain after the peak stress. The relationship between the plastic strains is used to model the total strains relationship. Finally the new model is compared to the existing test results.

A Khajeh Samani is PhD Student at the University of New South Wales (e-mail: ali.samani@unsw.edu.au).
Mario M. Attard is associate professor at the University of New South Wales (e-mail: m.attard@lunsw.edu.au).

II. Existing Models

The only analytical models studied here are those in which the lateral strains or volumetric strains are directly linked to the axial strain. The first model reviewed is that by [4]. In their model the ε' is the lateral strain and is given by.

$$\frac{\varepsilon'}{\varepsilon_0'} = v_i^a \left(\frac{\varepsilon}{\varepsilon_0}\right) \quad \varepsilon \le \varepsilon_1 \quad \text{or} \quad \left(\frac{\varepsilon}{\varepsilon_0}\right)^a \quad \varepsilon > \varepsilon_1 \tag{1}$$

Where:

$$v_i^a = 8\times10^{-6}\left(f_c'\right)^2 + 0.0002 f_c' + 0.138$$
$$a = 0.0177 f_c' + 1.2818 \tag{2}$$
$$\varepsilon_1 = \frac{\varepsilon_0.\ln\left(v_i^a\right)}{a-1}$$

In which ε is the axial strain, f_c' is the uniaxial compressive strength of concrete, ε_0' is the lateral strain at the peak stress and is equated to $0.5\varepsilon_0$, ε_0 is the axial strain corresponding to the peak stress given by:

$$\varepsilon_0 = \varepsilon_c.\left[1+\left(17-0.06 f_c'\right)\left(\frac{f_r}{f_c'}\right)\right] \tag{3}$$

In the above, ε_c is the strain at the peak stress in uniaxial condition assumed to be 0.002 f_r is the lateral confinement on the specimen.

The other model studied is given in [7]. In this model the secant Poisson's ratio is used to correlate the lateral deformation with the axial deformation. The concrete behaviour in the lateral direction is defined by three regions namely the elastic, inelastic hardening and softening. In [7]'s model:

$$\varepsilon' = -\nu_s \varepsilon \tag{4}$$

In which ν_s is the secant Poisson's ratio defined by:

$$\nu_s = \nu_e \quad \varepsilon \le \varepsilon_e \tag{5}$$

$$\nu_s = \nu_l - \left(\nu_l - \nu_e\right)\exp\left[-\left(\frac{\varepsilon-\varepsilon_e}{\Delta}\right)^2\right] \quad \varepsilon > \varepsilon_e \tag{6}$$

Where, ν_e is the elastic Poisson's ratio of the concrete varying between 0.15 to 0.2. Expressions for ε_e, ν_l and Δ are defined as:

$$\varepsilon_e = \frac{f_c'\left(0.1\sqrt{1+9.9\frac{f_r}{f_c'}}-0.9\left(\frac{f_r}{f_c'}\right)^2+\frac{f_r}{f_c'}\right)}{4750\sqrt{f_c'}} \quad (7)$$

$$\nu_l = \nu_p + \frac{1}{\left(\left(\frac{f_r}{f_c'}\right)+0.85\right)^4}$$

$$\Delta = \frac{\varepsilon_0 - \varepsilon_e}{\sqrt{-\ln\left(\frac{\nu_l-\nu_p}{\nu_l-\nu_0}\right)}} \quad (8)$$

Here, ν_p is the ratio of lateral strain to the axial strain at the peak stress and assumed to be 0.5, ν_l is the largest secant ratio. The axial strain at the peak stress that is given by:

$$\varepsilon_0 = 5.\left(-0.067 f_c'^2 + 29.9 f_c' + 1053\right) .\left(\left(\sqrt{1+9.9\frac{f_r}{f_c'}}+\frac{f_r}{f_c'}\right)-0.8\right)\times 10^{-6} \quad (9)$$

III. Comparing Existing Models with Experimental Results for Confined Concrete

In this section, the two models described above are compared to some of the experimental results available in the literature. The first set of results are those of [8] who tested concrete in triaxial and uniaxial compression in three different batches. The cylindrical specimens had a diameter of 54 mm and a height of 115 mm. The uniaxial compression strength was approximately 64.7, 43.5 and 21.2 MPa. In the triaxial tests, a confining pressure up to the desired level was first applied to the specimen and then the axial displacements were transmitted to the sample. The applied confinement levels varied from 0 MPa to 51.2 MPa. The lateral strains versus the total axial strain obtained from these tests are plotted in Fig. 1 & Fig. 2. In Fig. 1and Fig. 2 the comparison with the models proposed in [7] and [4] are also presented.

The second major set of test results used for the comparison, here, are those given in [9-10] in which tests results are presented for normal strength concrete in direct tension, uniaxial compression and triaxial compression. All tests were carried out in a servo controlled testing frame. The ultimate uniaxial compressive strength of the concrete was 22 MPa. The size of the cylindrical specimens in the uniaxial compression tests, were 76mm by 152 mm, while in the triaxial and the tensile tests, the specimens had a diameter of 54mm and a height of 108 mm. The tensile strength was approximately 2.53 MPa. A modified Hoek cell was used to impose the targeted confinement pressure on the triaxial specimens. The confining pressures ranged from 0.69 MPa to 13.79 MPa. The axial displacements were transmitted via steel rams without any friction reduction measures. The study in reference [10] highlighted that the unconfined compression tests exhibited the biggest dilatancy in the post peak regime, with radial displacements three times greater than the applied axial displacements. The results presented in reference [9] showed a large volumetric expansion in the post peak region. Similar to results presented in [6], [10]'s results showed that as the level of confinement was increased the dilatancy showed a rapid decrease while exhibiting a transition from large volumetric expansions under low confinement to an elastic volumetric compaction for the high confinement levels. Fig. 3 and Fig. 4 show the test results and the comparison with the predictions of models described in part I.

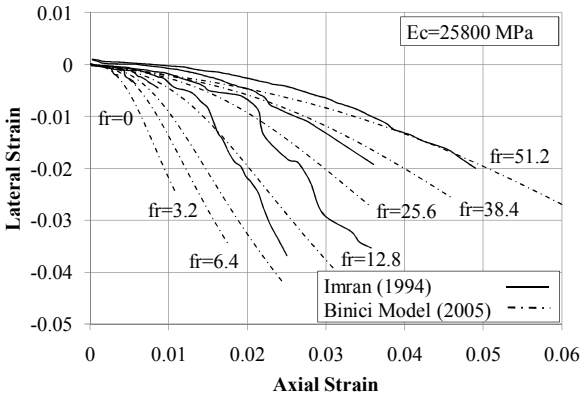

Fig. 1 Comparison of [8] test results (f'c=64.7 MPa) with [7] model

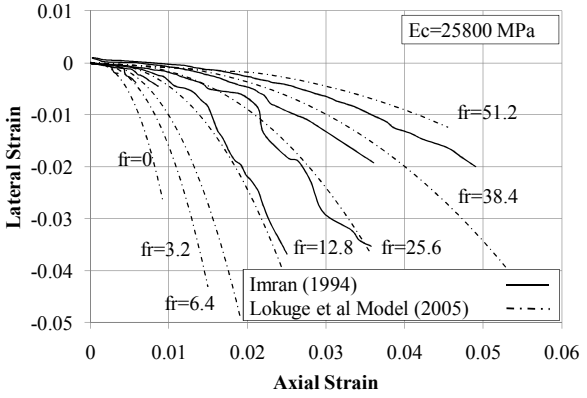

Fig. 2 Comparison of [8] test results (f'c=64.7 MPa) with [4] model

In all comparisons, the elastic modulus from the experimental results was used in the analytical models and the values of the axial strain at the peak stress was taken from experimental results rather than the empirical prediction. It can be seen that the models do not match the test results very well but provide a qualitative prediction. Moreover, none of the models are capable of predicting the behaviour of concrete under very high confinement level. In Fig. 4, when the confining pressure increases to 13.67 MPa, the specimen initially experiences compaction in the lateral direction before it starts to expand under axial compressive force but none of

the reviewed models are capable of predicting this behaviour at initial stage of tests.

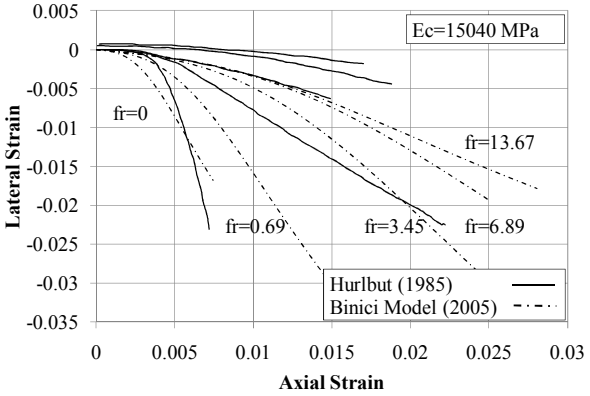

Fig. 3 Comparison of [10] test results with [7] model

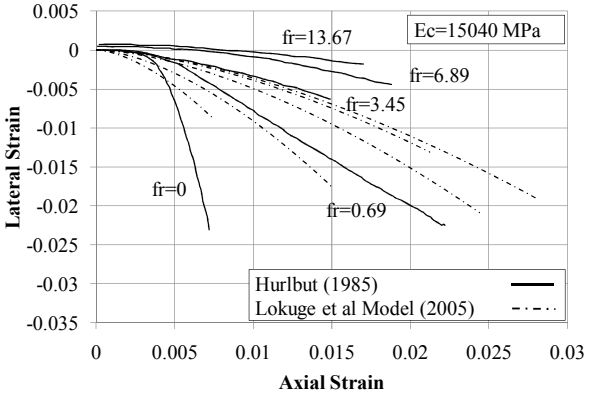

Fig. 4 Comparison of [10] test results with [4] model

IV. Stress Strain Model Proposed in [11]

Reference [11] proposed an axial stress versus axial strain model for confined concrete which will be used here to estimate the axial stress level, the peak axial stress, the axial strain corresponding to the peak stress and the concrete elastic modulus. The ascending branch of the stress strain curve can be represented by the following equation which was originally proposed by [5].

$$\frac{f}{f_0}=\frac{A.X+B.X^2}{1+C.X+D.X^2},$$

$$where\ X=\frac{\varepsilon}{\varepsilon_0} \tag{10}$$

$$\varepsilon_0\geq\varepsilon\geq 0,\quad 0\leq\frac{f}{f_0}\leq 1$$

In the above equation, f is the stress at the axial strain ε while f_0 is the peak stress at the axial strain ε_0. The constants A, B, C and D for the ascending curve are defined by:

$$A=\frac{E_{ti}\varepsilon_0}{f_0},$$

$$B=\frac{(A-1)^2}{\alpha_t\left(1-\frac{f_{pl}}{f_0}\right)}+\frac{A^2(1-\alpha_t)}{\alpha_t^2\frac{f_{pl}}{f_0}\left(1-\frac{f_{pl}}{f_0}\right)}-1, \tag{11}$$

$$C=(A-2),\quad D=(B+1)$$

$$with\ either\ B\geq 0\ \ or\ |B|<A$$

In the above, E_{ti} is the initial tangent modulus at zero stress and $\alpha_t = E_{ti}/E_c$, where E_c is the secant modulus of the concrete measured at a stress level of f_{Pl} (usually $0.45f_0$). The secant modulus is defined by (12) for stronger crushed aggregates or (13) for mixes containing weaker aggregates, such as vesicular basalt.

$$E_c=0.043\rho^{1.5}\sqrt{f_c'} \tag{12}$$

$$E_c=\left(3320\sqrt{f_c'}+6900\right)\left(\frac{\rho}{2320}\right)^{1.5} \tag{13}$$

For the softening descending branch, a power function is used with the condition that the stress strain curve passes through a point on the softening branch referred to as the inflexion point (f_i,ε_i) in [5]. The proposed post peak softening power function is:

$$\frac{f}{f_0}=\frac{f_{residual}}{f_0}+\left(1-\frac{f_{residual}}{f_0}\right)\left(\frac{f_{ic}}{f_c'}\right)^{\left(\frac{\varepsilon-\varepsilon_0}{\varepsilon_i-\varepsilon_0}\right)^2}\qquad \varepsilon\geq\varepsilon_0 \tag{14}$$

With $f_{residual}$ being the residual stress level ratio estimated from:

$$\frac{f_{residual}}{f_0}=1-\frac{1}{a\left(\frac{f_r}{f_c'}\right)^k+1},$$

$$a=795.7-3.291f_c', \tag{15}$$

$$k=\left(5.79\left(\frac{f_r}{f_c'}\right)^{0.694}+1.301\right)$$

The inflexion point stress ratio is given by:

$$\frac{f_i}{f_0}=\frac{f_{residual}}{f_0}+\left(1-\frac{f_{residual}}{f_0}\right)\left(\frac{f_{ic}}{f_c'}\right) \tag{16}$$

The uniaxial inflexion point $(f_{ic},\varepsilon_{ic})$ is estimated by:

$$\frac{f_{ic}}{f_c'}=1.41-0.17\ln\left(f_c'\right)$$

$$\frac{\varepsilon_{ic}}{\varepsilon_c}=2.76-0.35\ln\left(f_c'\right) \tag{17}$$

The inflexion point strain for the uniaxial case has been recalibrated from [5] proposal. Equation (14) reduces to the following for the post-peak softening branch for the uniaxial

state.

$$\frac{f}{f_c'}=\left(\frac{f_{ic}}{f_c'}\right)^{\left(\frac{\varepsilon-\varepsilon_c}{\varepsilon_{ic}-\varepsilon_c}\right)^2} \qquad \varepsilon_c \le \varepsilon \tag{18}$$

With ε_c being the uniaxial strain at the peak stress and is defined in [5]. The axial strain at the peak stress, ε_0, has also been recalibrated, and is given by:

$$\frac{\varepsilon_0}{\varepsilon_c}=e^k,$$
$$\mathrm{k}=\left(2.843-0.0014 f_c'\right)\left(\frac{f_r}{f_c'}\right)^{\left[0.579-0.099\left(\frac{f_r}{f_c'}\right)\right]} \tag{19}$$

A similar interpolation function to that in (16) can be devised for the inflexion point strain ratio, that is:

$$\frac{\varepsilon_t}{\varepsilon_0}=\frac{f_{residual}}{f_0}k+\left(1-\frac{f_{residual}}{f_0}\right)\left(\frac{\varepsilon_{ic}}{\varepsilon_c}\right),$$
$$k=1.26+\frac{2.89}{\sqrt{f_c'}} \tag{20}$$

Where the parameter k defining the limiting value for the inflexion point ratio as $f_{residual} \rightarrow f_0$.

V. Proposed Lateral Strain Model

The model for lateral strain as a function of the axial strain proposed here is:

$$\varepsilon' = \frac{\mu_e.f}{E_c}-\frac{f_r}{E_c}=\frac{\mu_e.f-f_r}{f-\mu_e.f_r}.\varepsilon \qquad \varepsilon \le \varepsilon_{pr} \tag{21}$$

$$\varepsilon' = \left[\frac{\mu_e f}{E_c}-\frac{f_r}{E_c}\right]+ \qquad \varepsilon_{pr} < \varepsilon \le \varepsilon_0$$
$$\left[\mu_0\varepsilon_0-\left[\frac{\mu_e f_0}{E_c}-\frac{f_r}{E_c}\right]\right]\times \tag{22}$$
$$\frac{\left(\frac{\varepsilon-\varepsilon_{pr}}{\varepsilon_o-\varepsilon_{pr}}\right)^2.\exp\left(\alpha.\left(\frac{\varepsilon-\varepsilon_{pr}}{\varepsilon_o-\varepsilon_{pr}}\right)\right)}{\exp(\alpha)}$$

$$\varepsilon' = \mu_e.\frac{f}{E_c}+ \qquad \varepsilon > \varepsilon_0$$
$$\beta.\left[\varepsilon-\frac{f}{E_c}-\left(\varepsilon_0-\frac{f_0}{E_c}\right)\right]+\mu_0\varepsilon_0-\mu_e.\frac{f_0}{E_c} \tag{23}$$

In which, μ_e is the elastic Poison ratio normally lying between 0.15 and 0.25. f is axial stress. f_{pr} and ε_{pr} are the axial stress and strain at the proportional limit taken roughly to occur at an axial stress level of 45% of the peak stress, f_0. E_c is the elastic modulus and is assumed to be equal to f_{pr}/ε_{pr} and is defined by either (12) or (13). ε_0 is the axial strain at the peak stress defined by (19). μ_0 is the ratio of the lateral strain to the axial strain at the peak stress. Based on study presented in [6], μ_0 assumed to be 0.5. β coefficient is based on a regression analysis of several experimental results ([10]-[12-16]) shown in Fig. 5 and is defined by (24). β is independent of axial strain variation and is therefore taken as a constant for a particular confinement level, in lateral strain versus axial strain relationship, and finally α is defined as:

$$\beta=\frac{-2}{12\times\left(\frac{f_r}{f_c'}\right)+1}-0.5$$
$$\alpha=\left(\frac{\beta}{\varepsilon_{P0}'}-2\right)\times\left(\varepsilon_o-\varepsilon_{pr}\right) \tag{24}$$

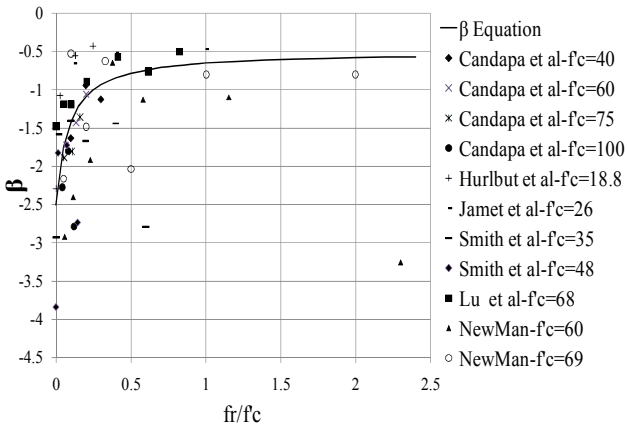

Fig. 5 β variation with confinement level

Fig. 6 to Fig. 8 show a comparison of the proposed model with test results of [6]-[8]-[10]-[12]. The proposed model predictions are generally very good and demonstrate the capability of the proposed model for a wide range of compressive strengths and confining pressures.

The volumetric strain is also used to show the behaviour of concrete in lateral direction. To measure the volumetric strain in the confined concrete tests, either changes in confining liquid volume are recorded or the sum of axial strain and two times the lateral strain is used. In this paper as the changes in confining liquid volume is not available, the sum of strains are used. There is no need to mention that the accuracy of the volumetric strain presented as test results depends on the accuracy of the measurement method. The comparison of the volumetric strain for test result of [12] with the volumetric strain obtained from the proposed model is very good and the model predicts the trend of the volumetric strains obtained from the tests of [13] and [9].

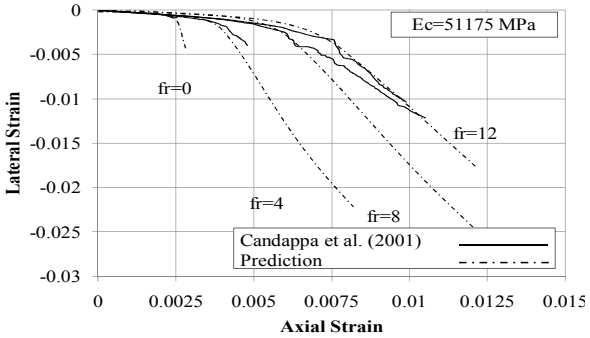

Fig. 6 Comparison of the lateral strain Vs. axial strain for [12] test results (f'c=100 MPa) with Proposed Model

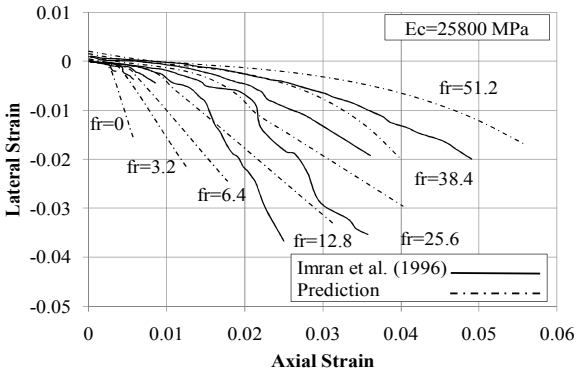

Fig. 7 Comparison of the lateral strain Vs. axial strain for [8] test results (f'c=64.7 MPa) with Proposed Model

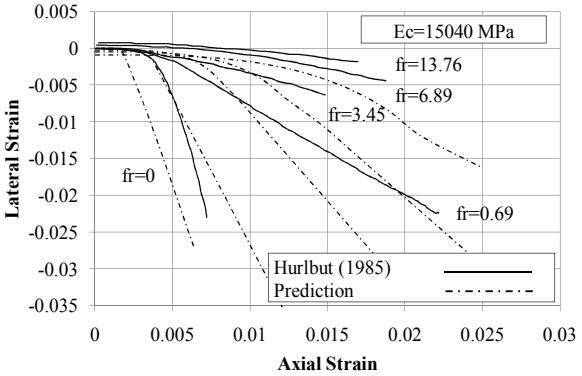

Fig. 8 Comparison of the lateral strain Vs. axial strain for [10] test results with Proposed Model

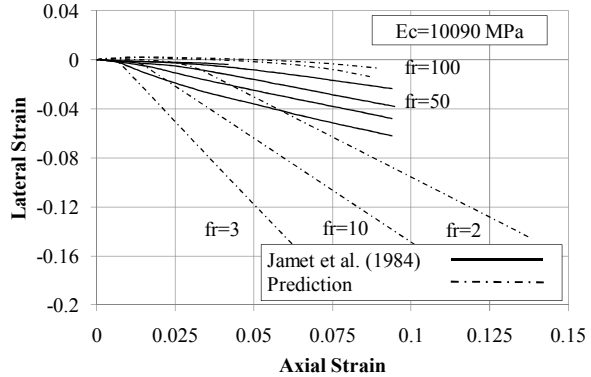

Fig. 9 Comparison of the lateral strain Vs. axial strain for [13] test results with Proposed Model

VI. Conclusion

The two analytical models for lateral strain versus axial strain proposed by [4]-[7] are reviewed and compared with tests results. The correlation between the test results and the analytical model prediction is not particularly high especially for very high confinement levels. The initial compaction under high confinement is not predicted with the mentioned models.

A new model for the lateral strain versus axial strain relationship has been proposed based on the assumption that the concrete behaviour could be classified into three regions. It was assumed that the concrete responds to loads linearly elastic up to a proportional limit and then its response changes to a nonlinear hardening up to the peak stress. From previous studies, the point at which the volumetric strain becomes zero corresponds to the peak stress point. Hence, by equating the volumetric strain to zero ($\varepsilon_a + 2\varepsilon_l = 0$), the lateral strain at the peak stress must be half the axial strain at the peak stress level. In the post peak region, a linear relationship between the plastic lateral strain and the plastic axial strain was observed. Since the elastic component of the lateral strain can be predicted from the elastic axial strain, the total lateral strain in post peak region could then be estimated from the sum of the predicted plastic and elastic lateral strains. The only parameter affecting this linear relationship between plastic lateral and axial strain was shown to be the confinement level.

To show the model's accuracy, the proposed model predictions were compared with a vast range of results in which the concrete strengths varied from low to high strength as well as varying confinement levels. The model showed a realistic match and displayed similar trends to those in the comparison experimental results.

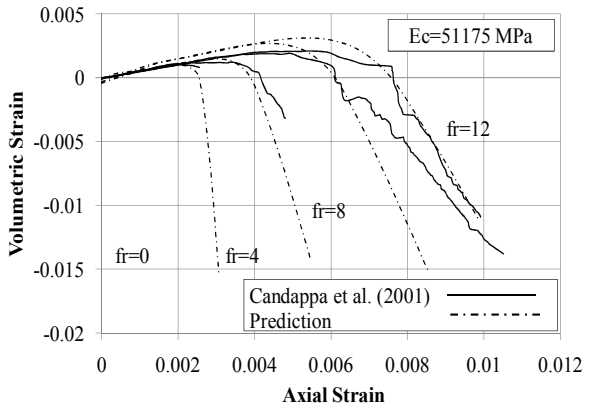

Fig. 10 Comparison of the volumetric strain Vs. axial strain for [12] test results (f'c=100 MPa) with Proposed Model

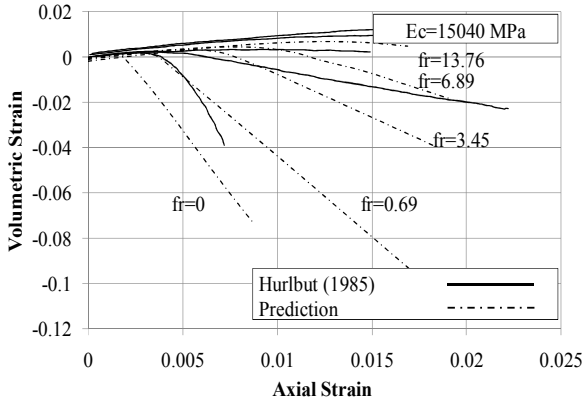

Fig. 11 Comparison of the volumetric strain Vs. axial strain for [9] test results with Proposed Model

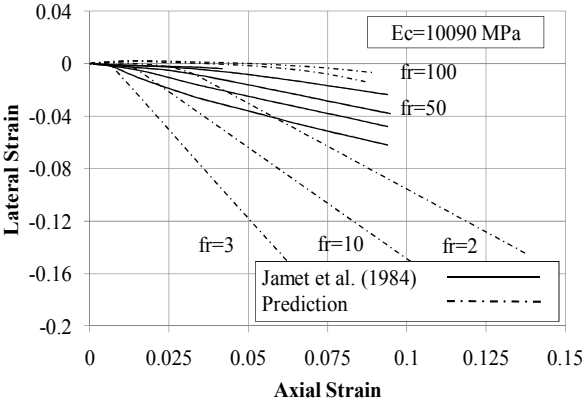

Fig. 12 Comparison of the volumetric strain Vs. axial strain for [13] test results with Proposed Model

REFERENCES

[1] Cusson, D. and P. Paultre, *Stress-strain model for confined high-strength concrete.* Journal of Structural Engineering, 1995. **121**: p. 468.

[2] Ahmad, S. and S. Shah, *Stress-strain curves of concrete confined by spiral reinforcement.* ACI Journal, 1982. **79**(6): p. 484-490.

[3] Talaat, M. and K. Mosalam, *Computational modeling of progressive collapse in reinforced concrete frame structures.* 2007: University of California, Berkeley.

[4] Lokuge, W., J. Sanjayan, and S. Setunge, *Stress–Strain Model for Laterally Confined Concrete.* Journal of Materials in Civil Engineering, 2005. **17**: p. 607.

[5] Attard, M. and S. Setunge, *Stress-strain relationship of confined and unconfined concrete.* ACI Materials Journal, 1996. **93**(5).

[6] Imran, I. and S. Pantazopoulou, *Experimental study of plain concrete under triaxial stress.* ACI Materials Journal, 1996. **93**(6): p. 589-601.

[7] Binici, B., *An analytical model for stress–strain behavior of confined concrete.* Engineering structures, 2005. **27**(7): p. 1040-1051.

[8] Imran, I., *Applications of non-associated plasticity in modeling the mechanical response of concrete.* University of Toronto, 1994.

[9] Willam, K., B. Hurlbut, and S. Sture, *Experimental and constitutive aspects of concrete failure.* Finite Element Analysis of Reinforced Concrete Structures (Proceedings of the Seminar sponsored by the Japan Society for the Promotion of Science and the U.S. National Science Foundation), 1986: p. 226-254.

[10] Hurlbut, B., *Experimental and computational investigation of strain-softening in concrete.* 1985, University of Colorado.

[11] Samani, A. and M. Attard, *A Stress-Strain Model For Uniaxial Compression And Triaxially Confined Plain Concrete Incorporating Size Effect*, in *UNICIV Report R-457*. 2010, The University of New South Wales, School of Civil and Environmental Engineering, Kensington,Sydney, Australia.

[12] Candappa, D., J. Sanjayan, and S. Setunge, *Complete triaxial stress-strain curves of high-strength concrete.* Journal of Materials in Civil Engineering, 2001. **13**: p. 209.

[13] Jamet, P., A. Millard, and G. Nahas, *Triaxial behaviour of micro-concrete complete stress-strain curves for confining pressures ranging from 0 to 100 MPa.* RILEM-CEB International conference concrete under multiaxial conditions, 1984. **1**: p. 133-140.

[14] Smith, S., et al., *Concrete Over the Top--Or, is there Life After Peak?* ACI Materials Journal, 1989. **86**(5).

[15] Lu, X. and C. Hsu, *Stress-Strain Relations of High-Strength Concrete under Triaxial Compression.* Journal of Materials in Civil Engineering, 2007. **19**: p. 261.

[16] Newman, J., *Concrete under complex stress*, in *Developments in Concrete Technology-I*, F. Lydon, Editor. 1979. p. 151-219.